Timing Jitter Reduction in Semiconductor Lasers Induced by Optical Injection

MARÍA DUQUE GIJÓN[1], ANA QUIRCE[2], JORDI TIANA-ALSINA[3], CRISTINA MASOLLER[1,*], AND ÁNGEL VALLE[2]

[1] Departament de Física, Universitat Politécnica de Catalunya, Rambla Sant Nebridi 22, 08222 Terrassa, Barcelona, Spain
[2] Instituto de Física de Cantabria (IFCA), Universidad de Cantabria-CSIC, Avda. Los Castros s/n, E-39005, Santander, Spain
[3] Department de Física Aplicada, Facultat de Física, Universitat de Barcelona, Martí i Franquès 1, 08028 Barcelona, Spain
[*] cristina.masoller@upc.edu

Compiled September 15, 2023

We present an experimental study of the effect of continuous wave optical injection (OI) from a vertical-cavity surface-emitting laser (VCSEL) on the timing jitter of a gain-switched discrete-mode semiconductor laser (DML). Timing jitter was analyzed over a wide range of temperatures of the DML, which allowed tuning the detuning between the lasers emissions, and it was compared with the inter-pulse timing jitter. We have found that there is a range of detunings in which OI diminishes the jitter by 70% with respect to the jitter of the solitary DML. However, within this region, there are some detunings for which OI significantly increases the jitter.

http://dx.doi.org/10.1364/ao.XX.XXXXXX

1. INTRODUCTION

Reducing the timing jitter from a train of pulses is crucial for many optical applications. Optical techniques as time division multiplexing-based communication, all-optical signal generation and all-optical signal processing (optical analog to digital converters and optical clock recovery), rely on low timing jitter [1–5]. In addition, very recently measurement-device-independent Quantum Key Distribution (MDI-QKD) systems using optical injection (OI) from a semiconductor laser into a gain-switched semiconductor laser have been demonstrated. A reduction of timing jitter, induced by OI, is desirable in these types of MDI-QKD systems as it improves the interference visibility [6–8].

The aim of the timing jitter reduction has led to investigate cost-effective and power-effective solutions. Therefore, many researches have focused on the use of OI and feedback in semiconductor lasers in order to study the effects of dynamical instabilities on the pulse width, the timing jitter, and timing jitter reduction [9–18]. As an example, in [19, 20] it is reported an experimental study of the reduction on either the timing jitter and the pulse width of optical pulses from a gain-switched single mode VCSEL with OI coming from a tunable laser. By optimizing the OI wavelength, timing jitter reductions of 40% and 70%, in comparison to the jitter of the solitary laser, were reported in [19] and [20], respectively.

In this work. we experimentally investigate how continuous-wave (cw) OI from a master laser (that is a vertical-cavity surface-emitting laser, VCSEL) affects the timing jitter (TJ) of a gain-switched discrete mode semiconductor laser (DML, Injected Laser), and we compare it with the inter-pulse jitter (IPJ). We begin by defining in Sec. 2 TJ and IPJ, then Sec. 3. presents the experimental setup and the procedure to measure TJ and IPJ, Sec. 4 presents the results and Sec.5, the discussion and our conclusions.

2. TIMING JITTER AND INTER-PULSE TIMING JITTER

Timing jitter (TJ) accounts for the timing deviations of N pulses with pulse positions t_n relative to an ideal pulse train, $\{\Delta t_n = t_n - nT_c\}$, being T_c the clock period. It represents the deviation from the ideal timing of each pulse fixed by an external clock (in our case, the injected laser current modulation). Specifically, timing jitter is quantified by the standard deviation of the distribution of $\{\Delta t_n\}$ values, TJ= $\sigma_{\Delta t}$.

On the other hand inter-pulse jitter (IPJ) quantifies the time variability of the times between pulses and is defined as the standard deviation of the distribution of time intervals between consecutive pulses, $\Delta T_n = t_n - t_{n-1}$, i.e., IPJ= $\sigma_{\Delta T}$.

3. EXPERIMENTAL SETUP AND PROCEDURE

The experimental all-fiber setup is shown in Fig. 1. A 1550 nm InAlGaAs VCSEL (RayCan) with 1.9 mA threshold at 35 ºC that operated in continuous wave mode was unidirectionally coupled to a DML (Eblana Photonics EP1550-0-DM-H19- FM, MQW laser in a ridge waveguide with index perturbations for single-mode operation), with 14.28 mA threshold at 27 ºC.

Temperature and injection current of the VCSEL were controlled with an accuracy of 0.01 ºC and 0.01 mA (Thorlabs TED200C and LDC200C), while temperature and injection current control of the DML were carried out by the laser drivers Luzwavelabs LDC/E-Temp3 and Luzwavelabs LDC/E-Current200, respectively, with an accuracy of 0.01 ºC and 0.01 mA. In addition, a sinusoidal signal modulation from a signal generator (SG, Keysight-N5173B) was added via a bias-tee to

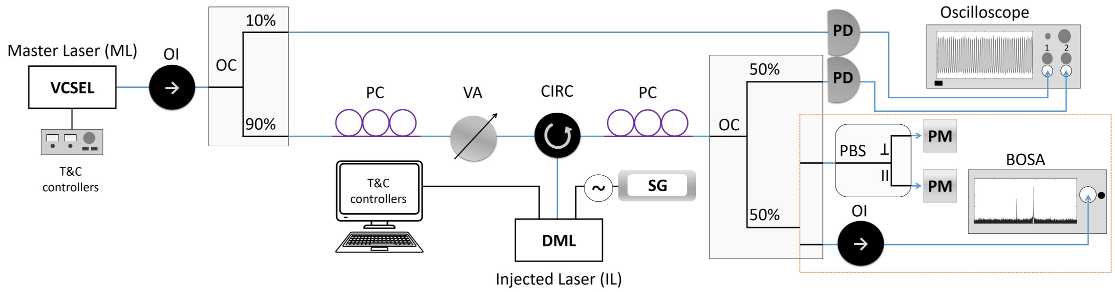

Fig. 1. Experimental setup: a VCSEL (Master Laser) provides cw optical injection to a DML (Injected Laser). BOSA: Brillouin Optical Spectrum Analyzer, CIRC: Circulator, T&C: Temperature and Current, OC: Optical Coupler, OI: Optical Isolator, PBS: Polarization Beam Splitter, PC: Polarization Controller, PD: Photo Diode, PM: Power Meter, SG: Signal Generator, VA: Variable Attenuator.

the bias injection current of the DML in order to generate an optical comb in gain-switching mode (as in previous studies [21]). A 90/10 Optical Coupler (OC) divided the principal beam emitted by the ML; while the 90% of the incoming light was injected into the DML through an optical circulator, the remaining 10% was analysed in the Oscilloscope (Keysight (Agilent) DSO91204A). Two polarization controllers (PC) and a polarization beam splitter (PBS), were used in order to maximize the optical coupling between the two lasers, while the amount of light that was injected into the DML was controlled by a variable attenuator (VA). With an Optical Circulator (CIRC) and a second 50/50 OC, the DML signal, either under solitary or injection configuration was analysed in the Oscilloscope. The other port of the OC was used either to assure parallel OI into the DML, or to analyse its optical spectra with a Brillouin Optical Spectrum Analyser (BOSA, Aragon Photonics BOSA 210). We were also able to measure the optical spectra and the polarization state of the ML though a back-reflection at the front facet of the DML. The optical signals from the lasers were electrically converted by two fast-photodiodes (PD, 9 GHz bandwidth, Thorlabs PDA8GS) and analysed in the Oscilloscope. In order to avoid back reflections, two optical isolators were positioned after the VCSEL and before the BOSA. Timing jitter, inter-pulse timing jitter and FWHM (full width at half maximum) were calculated, with a post processing analysis in MATLAB, with the time series of the gain-switched optically injected DML extracted from the Oscilloscope with a sampling rate of 40 GSa/s.

The VCSEL current and temperature were kept constant at 5 mA and 35 ºC respectively. The DML current was set at 30 mA and its temperature was varied from 15.04 ºC to 30 ºC in steps of 0.08 ºC. A sinusoidal modulation signal with a frequency of 5 GHz and a voltage amplitude of 1.5 V was added during the measurements.We have chosen the value of 5 GHz for the modulation frequency because it is close to the relaxation oscillation frequency at 30 mA bias current. The amplitude, 1.5 V, was chosen in order to drive the laser to low levels, where light emission is dominated by spontaneous emission noise.

4. RESULTS

Figures 2(a, d, g) display three examples of time series of the DML output for T_{DML} = 18.96 ºC in the solitary case and under injection for T_{DML} = 18.96 ºC and 19.84 ºC, respectively. Blue dots represent the threshold crossings that define the pulse times, $\{t_n\}$, from which the timing jitter (TJ) and the inter-pulse jitter (IPJ) were calculated. TJ is calculated from the histograms shown in Fig. 2(b, e, h), while IPJ, from the histograms in (c, f, i). In these histograms, the blue lines indicate the standard deviations from their respective mean values, in red. We see clear differences in the shape of the TJ and IPJ distributions that indicate that these measures are not equivalent. The TJ measure tracks the temporal position of a single pulse relative to the clock, accounting for only one source of variability. In contrast, the IPJ measures the time difference between two consecutive pulses, each with its own source of variability. As a result, we expect higher IPJ values compared to TJ.

For the solitary DML at 18.96 ºC, Fig. 2 (a), the laser output is almost periodic; therefore, Δt_n (b) and ΔT_n (c) histograms are well centered around their mean values. However, for the injected DML, the laser output is even more regular, Fig. 2 (d), and the histograms of Δt_n (e) and ΔT_n (f) are narrower. Therefore, for this temperature, OI effectively reduces TJ and IPJ with respect to the solitary values.

However, we have found that there are conditions in which OI does not reduce but increases TJ and IPJ. An example is shown in Fig. 2(g), where we see in the DML output, a period-doubling type of oscillation in the envelope of the pulses, which leads to the bimodal histograms shown in panels (h) and (i), and therefore, to an increase of TJ and IPJ. An injected semiconductor laser exhibits a rich variety of dynamical regimes [22], which are in part due to the phase-amplitude coupling (non-zero alpha factor), and in particular, period-doubling oscillations in the envelope of the pulses have been recently discussed in [23].

Figure 3 displays TJ (a) and IPJ (b) of the solitary and injected DML as a function of its temperature, and (top horizontal axis) the detuning, $\Delta\nu = \nu_{ML} - \nu_{DML}$, where ν_{ML} and ν_{DML} are the continuous wave wavelengths of the VCSEL and the DML, respectively, measured with the BOSA. The symbols indicate the TJ and IPJ values for the temperatures analysed in Fig. 2.

For the solitary laser, both TJ and IPJ increase with the temperature. This is explained since the squared TJ is roughly proportional to the inverse of the differential gain, G_N [24], and G_N decreases when increasing the temperature. When the DML is optically injected, there is a wide detuning range in which TJ and IPJ are significantly reduced. An example of this situation was shown in Figs. 2(a-f) and corresponds to the cyan and green symbols in Figs. 3(a, b). In this case, applying OI to the DML, TJ is reduced from 2.60 to 0.98 ps and IPJ from 3.93 to 0.95, resulting in reductions of 62% and 75%, respectively. Reductions can be larger (up to 70% and 79% of TJ and IPJ) for higher T_{DML}.

However, within this range, for particular temperatures, the TJ and IPJ increase with respect to the solitary values. The violet star in Fig. 3(a,b) indicates an example case, shown in Figs. 2(g-i). As explained before, OI induces a small modulation in the

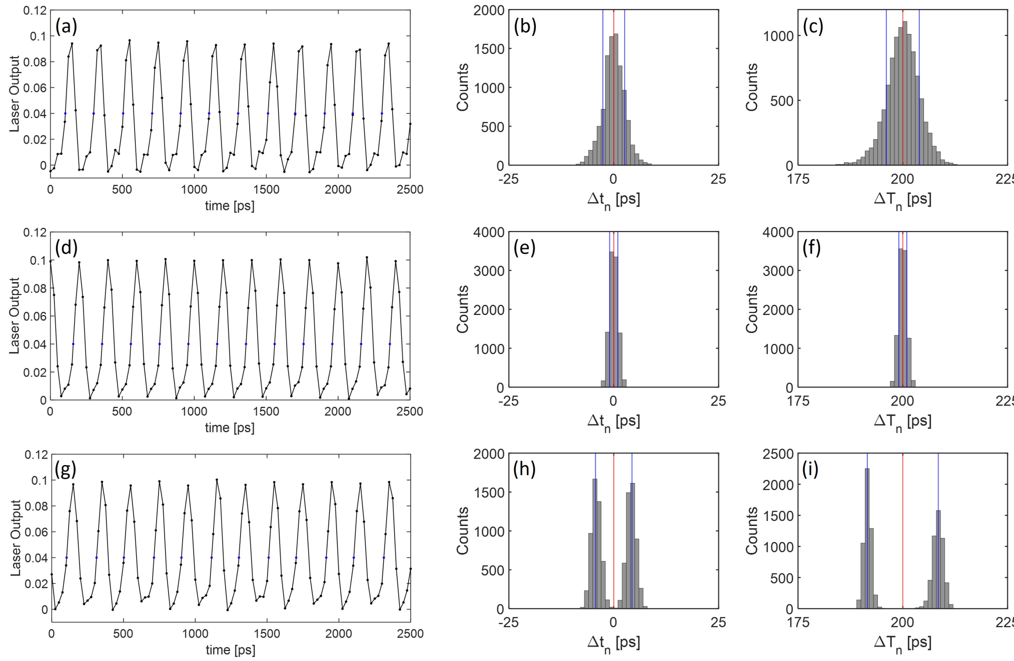

Fig. 2. (a,d,g) Examples of DML time series. Histograms of (b, e, h) Δt_n and of (c, f, i) ΔT_n for the solitary laser (a, b, c) with T_{DML} = 18.96 ºC and for the injected laser with T_{DML} = 18.96 ºC (d, e, f) and T_{DML} = 19.84 ºC (g, h, i). In panels (a,d,g), blue dots indicate the threshold used to detect the pulse times $\{t_n\}$.

envelope of the pulses that results in bimodal histograms in Fig. 2(h) and Fig. 2(i), and, in consequence, IN larger TJ and IPJ values. As expected, if the detuning is sufficiently large (positive or negative), there is no noticeable effect of OI and the TJ and IPJ are the same for the solitary and for the injected laser.

TJ and IPJ of the injected laser as a function of $\Delta\nu$ are compared in Fig. 3(c). It is shown that inter-pulse timing jitter is larger than timing jitter for the considered $\Delta\nu$ range. We also include the dependence of the FWHM with $\Delta\nu$. For each temperature, FWHM is calculated by averaging the FWHM of all the pulses. We see that the pulse width increases in the center of the region when jitter experiences a maximum reduction (small negative $\Delta\nu$). The effect of optical injection on FWHM is consistent with previous work, as large values of FWHM have been reported when decreasing the frequency of the signal (see Figs. 6 and 7 in [20]). This effect can be understood because the timing jitter and the FWHM are anticorrelated [25].

These results qualitatively confirm the simulations in [26, 27]. We remark that the peaks of TJ and IPJ observed in Fig. 3 that appear inside the $\Delta\nu$ region in which TJ and IPJ are reduced due to the optical injection were not observed in previous experimental studies [20, 25, 28], while they were predicted in [26, 27].

Jitter reduction by OI can be interpreted as follows. The sinusoidal variation of the DML current induces non-sinusoidal variations of the carrier density. The emission frequency follows the variations of the carrier density due to the carrier density dependence of the refractive index. This dynamic chirp, proportional to the alpha factor, is a transient phenomenon primarily causing the spectral broadening. When OI is applied close to the solitary DML frequency a transient frequency locking occurs in which the frequency of master and slave laser are equal and the chirp is significantly lower than the solitary laser chirp [26]. The range of detunings giving rise to transient frequency locking defines the dynamical locking range that can be much broader than the cw-locking range. Jitter reduction with OI is observed in the dynamical locking range, attributing it to the transient frequency locking.

However, OI can significantly increase the jitter, as theoretically reported in [23] (see Fig. 5). Our measurements indicate that these localized jitter increases can be associated to the appearance of period-doubling oscillations in the pulse envelope. When the DML's temperature increases, the threshold current increases and the differential gain decreases. Both situations increase the jitter of the solitary DML. A decrease of the differential gain increases the jitter [24] as it has been already discussed in the manuscript. An increase of the threshold current, for a fixed bias current, leads to a decrease of the bias current with respect to the threshold, and as discussed in point 1, the value of the jitter of the solitary laser increases. When OI is applied the value of the jitter, with the exception of the localized increases, is rather constant (see Fig. 3, or Fig. 5 in [26], or Figs. 6 and 7 in [20]). This is because the jitter reduction is due to transient frequency locking, that is a phenomenon observed, in our experiment, for temperatures between 19^{o}C and 23^{o}C. Far from that locking range, the OI effect is not relevant since a monotonous increase of the jitter with the temperature is observed, which is consistent with the variation for the solitary DML. This is confirmed in Fig. 3 by the similar values of jitter in the solitary and OI laser for large values of the temperature.

We conclude the discussion of the results by remarking that the specific range of detunings where jitter reduction can be obtained depends on the bias currents of the lasers, because an increase of the VCSEL current will not only increase the injection strength (the ratio of injected power/slave laser power), but also, it will modify the detuning. On the other hand, an increase of the DML current will decrease the injection strength, and it will also modify the detuning (in the opposite way as when the VCSEL's bias current increases).

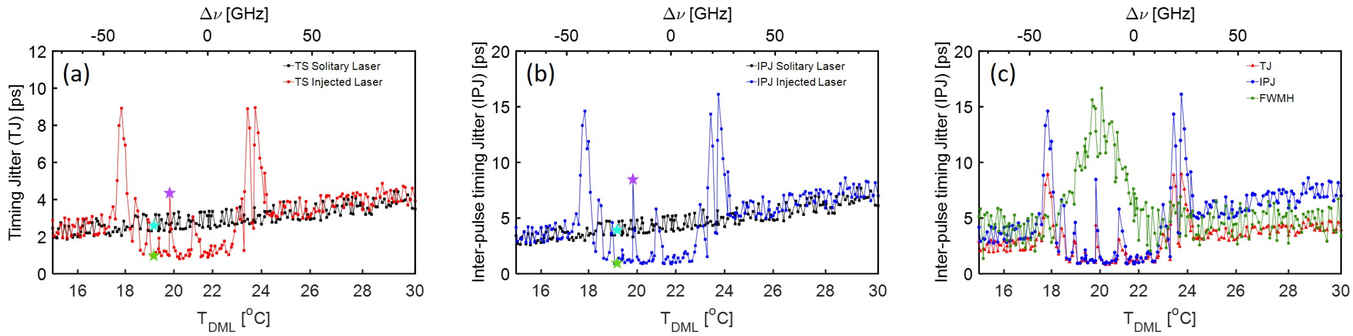

Fig. 3. (a) Comparison of the timing jitter (TJ) of the solitary (black line) and injected (red line) laser. (b) Inter-pulse timing jitter (IPJ) for the solitary and injected (blue line) laser. (c) Timing jitter, inter-pulse timing jitter and FWHM (green line) for the injected laser. Cyan, green and violet symbols in panels (a) and (b) refer to the points analyzed in Fig. 2.

5. CONCLUSIONS

We have experimentally studied the effect of optical injection (OI) in the timing jitter (TJ) of a gain-switched laser. We have shown that within the detuning region in which that TJ reduction is observed there are detuning values for which large values of the jitter are observed. This is seen for instance in Fig. 3(a) at -20 GHz detuning (violet star): the TJ increases with OI, being twice the TJ value of the solitary laser. This result can have impact on MDI-QKD systems since a careful choice of the detuning needs to be done in order to ensure that the jitter decreases. The comparison of our observations with early numerical predictions [26, 27] is good and to the best of our knowledge this is the first time that these localized jitter increases are experimentally observed.

We have also compared the TJ with the inter-pulse timing jitter (IPJ) and found that their variation with the DML temperature (that in turn, varies the detuning) is qualitatively the same. TJ presents lower values than IPJ, except for small detunings. At these detunings, both values reach their minimum and overlap. In this region, FHWM reveals an increase in the width of the pulses, reaching 74.7 ps. This experimental observation is in good qualitative agreement with the model simulations presented in [26, 27].

Acknowledgments. This work was supported by AGAUR (2021 SGR 00606 and FI scholarship), ICREA Academia, Ministerio de Ciencia e Innovación (PID2021-123994NB-C21 and PID2021-12345OB-C22 MCIN/AEI/FEDER UE), and Beatriz Galindo program (Ministerio de Ciencia, Innovación y Universidades).

Disclosures. The authors declare no conflicts of interest.

Data availability. Data underlying the results presented in this paper may be obtained from the authors upon reasonable request.

REFERENCES

1. D. Tong, B. Mikkelsen, T. Nielsen, K. Dreyer, and J. Johnson, IEEE Photonics Technol. Lett. **12**, 1064 (2000).
2. S. Zhang, F. Gomez-Agis, Y. Liu, N. Calabretta, E. Tangdiongga, and H. J. S. Dorren, Opt. Lett. **35**, 37 (2010).
3. J. Renaudier, B. Lavigne, P. Gallion, and G. H. Duan, J. Light. Technol. **24**, 3734 (2006).
4. O. Brox, S. Bauer, M. Biletzke, H. Ding, J. Kreissl, H.-J. Wünsche, and B. Sartorius, "Self-pulsating dfb for 40 ghz clock-recovery: Impact of intensity fluctuations on jitter," in Optical Fiber Communication Conference, (Optica Publishing Group, 2004), p. MF55.
5. T. Mori et al., "Timing jitter reduction by all-optical regeneration using a polarization bistable vcsel," in 2006 Conference on Lasers and Electro-Optics and 2006 Quantum Electronics and Laser Science Conference, (2006), pp. 1–2.
6. T. K. Paraïso, R. I. Woodward, D. G. Marangon, V. Lovic, Z. Yuan, and A. J. Shields, Adv. Quantum Technol. **4**, 2100062 (2021).
7. V. Lovic, D. Marangon, M. Lucamarini, Z. Yuan, and A. Shields, Phys. Rev. Appl. **16**, 054012 (2021).
8. F. Xu, X. Ma, Q. Zhang, H.-K. Lo, and J.-W. Pan, Rev. Mod. Phys. **92**, 025002 (2020).
9. J. Mulet and J. Mork, IEEE J. Quantum Electron. **42**, 249 (2006).
10. C.-Y. Lin, F. Grillot, Y. Li, R. Raghunathan, and L. F. Lester, IEEE J. Sel. Top. Quantum Electron. **17**, 1311 (2011).
11. M. Mangold, S. M. Link, A. Klenner, C. A. Zaugg, M. Golling, B. W. Tilma, and U. Keller, IEEE Photonics J. **6**, 1 (2014).
12. C. Otto, L. Jaurigue, E. Schöll, and K. Lüdge, IEEE Photonics J. **6**, 1 (2014).
13. A. Pimenov, T. Habruseva, D. Rachinskii, S. P. Hegarty, G. Huyet, and A. G. Vladimirov, Opt. Lett. **39**, 6815 (2014).
14. Y. Mao, J. Liu, Z. Lu, C. Song, and P. Poole, IEEE J. Sel. Top. Quantum Electron. **PP**, 1 (2019).
15. Y. Mao, Z. Lu, J. Liu, P. J. Poole, and G. Liu, J. Light. Technol. **38**, 4787 (2020).
16. S. Meinecke and K. Lüdge, Appl. Phys. Lett. **118**, 011104 (2021).
17. Y. Mao, G. Liu, K. Zeb, Z. Lu, J. Liu, P. J. Poole, C.-Y. Song, and P. Barrios, Photonics **9**, 695 (2022).
18. L. Drzewietzki, S. Breuer, and W. Elsäßer, Opt. Express **21**, 16142 (2013).
19. S. H. Lee, K. H. Kim, V. M. Deshmukh, D. W. Kim, and M.-H. Lee, IEEE J. Quantum Electron. **46**, 1327 (2010).
20. A. Consoli et al., "Optical injection-induced timing jitter reduction in gain-switched single-mode vertical-cavity surface-emitting lasers," in Semiconductor Lasers and Laser Dynamics IV, , vol. 7720 (SPIE, 2010), pp. 108–117.
21. A. Rosado, A. Pérez-Serrano, J. M. G. Tijero, A. V. Gutierrez, L. Pesquera, and I. Esquivias, IEEE J. Quantum Electron. **55**, 1 (2019).
22. J. Ohtsubo, Semiconductor lasers: stability, instability and chaos, 3rd Ed. (Springer, 2012).
23. A. Quirce, A. Rosado, J. Diez et al., IEEE Photonics J. **12**, 1503314 (2020).
24. P. Spano, A. D'Ottavi, A. Mecozzi, B. Daino, and S. Piazzolla, IEEE J. Quantum Electron. **25**, 1440 (1989).
25. D. S. Seo, D. Y. Kim, and H. F. Liu, Electron. Lett. **32**, 44 (1996).
26. J. Dellunde, M. Torrent, J. Sancho, and M. San Miguel, IEEE J. Quantum Electron. **33**, 1537 (1997).
27. J. Noriega, A. Valle, and L. Pesquera, Opt. Quantum Electron. **40**, 119 (2008).
28. D.-S. Seo, H.-F. Liu, D. Y. Kim, and D. D. Sampson, Appl. Phys. Lett. **67**, 1503 (1995).

FULL REFERENCES

1. D. Tong, B. Mikkelsen, T. Nielsen, K. Dreyer, and J. Johnson, "Opto-electronic phase-locked loop with balanced photodetection for clock recovery in high-speed optical time-division-multiplexed systems," IEEE Photonics Technol. Lett. **12**, 1064–1066 (2000).
2. S. Zhang, F. Gomez-Agis, Y. Liu, N. Calabretta, E. Tangdiongga, and H. J. S. Dorren, "Fast-synchronization and low-timing-jitter self-clocking concept for 160 gbit/s optical time-division multiplexing transmissions," Opt. Lett. **35**, 37–39 (2010).
3. J. Renaudier, B. Lavigne, P. Gallion, and G. H. Duan, "Study of phase-noise properties and timing jitter of 40-ghz all-optical clock recovery using self-pulsating semiconductor lasers," J. Light. Technol. **24**, 3734–3742 (2006).
4. O. Brox, S. Bauer, M. Biletzke, H. Ding, J. Kreissl, H.-J. Wünsche, and B. Sartorius, "Self-pulsating dfb for 40 ghz clock-recovery: Impact of intensity fluctuations on jitter," in Optical Fiber Communication Conference, (Optica Publishing Group, 2004), p. MF55.
5. T. Mori et al., "Timing jitter reduction by all-optical regeneration using a polarization bistable vcsel," in 2006 Conference on Lasers and Electro-Optics and 2006 Quantum Electronics and Laser Science Conference, (2006), pp. 1–2.
6. T. K. Paraïso, R. I. Woodward, D. G. Marangon, V. Lovic, Z. Yuan, and A. J. Shields, "Advanced laser technology for quantum communications (tutorial review)," Adv. Quantum Technol. **4**, 2100062 (2021).
7. V. Lovic, D. Marangon, M. Lucamarini, Z. Yuan, and A. Shields, "Characterizing phase noise in a gain-switched laser diode for quantum random-number generation," Phys. Rev. Appl. **16**, 054012 (2021).
8. F. Xu, X. Ma, Q. Zhang, H.-K. Lo, and J.-W. Pan, "Secure quantum key distribution with realistic devices," Rev. Mod. Phys. **92**, 025002 (2020).
9. J. Mulet and J. Mork, "Analysis of timing jitter in external-cavity mode-locked semiconductor lasers," IEEE J. Quantum Electron. **42**, 249–256 (2006).
10. C.-Y. Lin, F. Grillot, Y. Li, R. Raghunathan, and L. F. Lester, "Microwave characterization and stabilization of timing jitter in a quantum-dot passively mode-locked laser via external optical feedback," IEEE J. Sel. Top. Quantum Electron. **17**, 1311–1317 (2011).
11. M. Mangold, S. M. Link, A. Klenner, C. A. Zaugg, M. Golling, B. W. Tilma, and U. Keller, "Amplitude noise and timing jitter characterization of a high-power mode-locked integrated external-cavity surface emitting laser," IEEE Photonics J. **6**, 1–9 (2014).
12. C. Otto, L. Jaurigue, E. Schöll, and K. Lüdge, "Optimization of timing jitter reduction by optical feedback for a passively mode-locked laser," IEEE Photonics J. **6**, 1–14 (2014).
13. A. Pimenov, T. Habruseva, D. Rachinskii, S. P. Hegarty, G. Huyet, and A. G. Vladimirov, "Effect of dynamical instability on timing jitter in passively mode-locked quantum-dot lasers," Opt. Lett. **39**, 6815–6818 (2014).
14. Y. Mao, J. Liu, Z. Lu, C. Song, and P. Poole, "Ultra-low timing jitter of quantum dash semiconductor comb lasers with self-injection feedback locking," IEEE J. Sel. Top. Quantum Electron. **PP**, 1–1 (2019).
15. Y. Mao, Z. Lu, J. Liu, P. J. Poole, and G. Liu, "Pulse timing jitter estimated from optical phase noise in mode-locked semiconductor quantum dash lasers," J. Light. Technol. **38**, 4787–4793 (2020).
16. S. Meinecke and K. Lüdge, "Efficient timing jitter simulation for passively mode-locked semiconductor lasers," Appl. Phys. Lett. **118**, 011104 (2021).
17. Y. Mao, G. Liu, K. Zeb, Z. Lu, J. Liu, P. J. Poole, C.-Y. Song, and P. Barrios, "Ultralow noise and timing jitter semiconductor quantum-dot passively mode-locked laser for terabit/s optical networks," Photonics **9**, 695 (2022).
18. L. Drzewietzki, S. Breuer, and W. Elsäßer, "Timing jitter reduction of passively mode-locked semiconductor lasers by self-and external-injection: Numerical description and experiments," Opt. Express **21**, 16142–16161 (2013).
19. S. H. Lee, K. H. Kim, V. M. Deshmukh, D. W. Kim, and M.-H. Lee, "Injection laser wavelength-dependent timing jitter reduction of gain-switched single-mode vcsels," IEEE J. Quantum Electron. **46**, 1327–1331 (2010).
20. A. Consoli et al., "Optical injection-induced timing jitter reduction in gain-switched single-mode vertical-cavity surface-emitting lasers," in Semiconductor Lasers and Laser Dynamics IV, vol. 7720 (SPIE, 2010), pp. 108–117.
21. A. Rosado, A. Pérez-Serrano, J. M. G. Tijero, A. V. Gutierrez, L. Pesquera, and I. Esquivias, "Numerical and experimental analysis of optical frequency comb generation in gain-switched semiconductor lasers," IEEE J. Quantum Electron. **55**, 1–12 (2019).
22. J. Ohtsubo, Semiconductor lasers: stability, instability and chaos, 3rd Ed. (Springer, 2012).
23. A. Quirce, A. Rosado, J. Diez et al., "Nonlinear Dynamics Induced by Optical Injection in Optical Frequency Combs Generated by Gain-Switching of Laser Diodes," IEEE Photonics J. **12**, 1503314 (2020).
24. P. Spano, A. D'Ottavi, A. Mecozzi, B. Daino, and S. Piazzolla, "Experimental measurements and theory of first passage time in pulse-modulated semiconductor lasers," IEEE J. Quantum Electron. **25**, 1440–1449 (1989).
25. D. S. Seo, D. Y. Kim, and H. F. Liu, "Timing jitter reduction of gain-switched dfb laser by external injection-seeding," Electron. Lett. **32**, 44–45 (1996).
26. J. Dellunde, M. Torrent, J. Sancho, and M. San Miguel, "Frequency dynamics of gain-switched injection-locked semiconductor lasers," IEEE J. Quantum Electron. **33**, 1537–1542 (1997).
27. J. Noriega, A. Valle, and L. Pesquera, "Timing jitter reduction in gain-switched vcsels induced by external optical injection," Opt. Quantum Electron. **40**, 119–129 (2008).
28. D.-S. Seo, H.-F. Liu, D. Y. Kim, and D. D. Sampson, "Injection power and wavelength dependence of an external-seeded gain-switched fabry–perot laser," Appl. Phys. Lett. **67**, 1503–1505 (1995).